

Electronic Supporting Information for

Crystal Phase of Nickel Sulfides Dictates Hydrogen Evolution Activity of Various Semiconducting Photocatalysts

Jianjian Yi^a, Yu Xia^a, Zhou Zhou^a, Ganghua Zhou^a, Xianglin Zhu^b, Sai Zhang^c, Xingwang Zhu^a, Xiaozhi Wang^{a,}, Hui Xu^{b,*}, and Huan Pang^{a,*}*

^a College of Environmental Science and Engineering, School of Chemistry and Chemical Engineering, Yangzhou University, Yangzhou, Jiangsu 225127, China

^b Institute for Energy Research, Jiangsu University, Zhenjiang, Jiangsu 212013, China

^c Department of Materials Science and State Key Laboratory of Molecular Engineering of Polymers, Fudan University, Shanghai 200433, China

* Corresponding authors:

xzwang@yzu.edu.cn (X. Wang); xh@ujs.edu.cn (H. Xu);

huanpangchem@hotmail.com, panghuan@yzu.edu.cn (H. Pang)

Material characterization

The crystal phase was performed by X-ray diffraction (XRD) on a Bruker D8 Advanced X-ray Diffractometer (Cu-K α radiation: $\lambda = 0.15406$ nm). The microstructures and morphology of samples were observed by field emission scanning electron microscopy (FE-SEM, S-4800II) under the acceleration voltage of 5.0 kV. High-resolution TEM (HRTEM) images and elemental mapping were captured on a Tecnai G2 F30 S-TWIN at an acceleration voltage of 300 kV. The light absorption capacity was tested by Cary 5000 UV-visible-near-infrared absorption spectrometer. X-ray photoelectron spectra (XPS) was obtained on a Thermo Scientific ESCALAB 250 apparatus. The photoluminescence (PL) spectra were obtained by Edinburgh FLS1000 fluorescence spectrometer.

Photo-electrochemical test

The photocurrents were measured by a CHI 660E electrochemical system, which was equipped with a standard three-electrode system. 2 mg of samples was dispersed in a solution containing 85 μL ethanol and 15 μL EG. Then 30 μL of the suspension was drop-casted onto an indiumtin oxide (ITO)-coated glass and dried on a 1 cm*1 cm area. In the experiment, an ITO with a sample on it was used as a working electrode. Pt wire was employed as the counter electrode and the reference electrode was Ag/AgCl/sat. KCl. A bias potential of -0.1V (vs. Ag/AgCl) was employed. Na_2SO_4 solution (0.1 M) was used as the electrolyte. The light source was a 300 W Xe lamp. The Mott-Schottky plots were also measured using the same three electrode system over an alternating current frequency of 1500 Hz in 0.1M Na_2SO_4 aqueous solution.

Theoretical simulation

The DFT calculations were carried out using the Vienna ab initio simulation package (VASP). The exchange-correlation energy was described using the (PBE). The Perdew-Burke-Ernzerhof (PBE) functional combined with Projected Augmented Wave (PAW) pseudopotentials was used. A 520 eV plane-wave kinetic energy cut off was selected, and a $3 \times 3 \times 1$ Monkhorst-Pack k point sampling was adopted for the structure relaxation. A $p(2 \times 2)$ supercell model with 15 Å vacuum in c-axis was employed to simulate the NiS_x . A residual force threshold of 0.05 eV \AA^{-1} was set for geometry optimizations. The calculated surface in (001) surface in model building process.

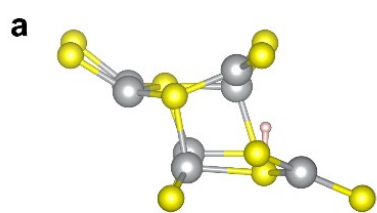
The Gibbs free-energy (ΔG_{H^*}) is expressed as: $\Delta G_{\text{H}^*} = \Delta E_{\text{H}^*} + \Delta E_{\text{ZPE}} - T\Delta S$. Where ΔE_{H^*} , ΔE_{ZPE} and ΔS are the adsorption energy of atomic hydrogen on the given surface, zero point energy correction and entropy change of H^* adsorption, respectively. The zero point energy correction can be estimated by the equation $\Delta E_{\text{ZPE}} = E_{\text{ZPE}}(\text{H}^*) - 1/2 E_{\text{ZPE}}(\text{H}_2)$. ΔS can be calculated by the equation $\Delta S = S(\text{H}^*) - 1/2 S(\text{H}_2) \approx -1/2 S(\text{H}_2)$, due to the negligible of the entropy of hydrogen in adsorbed state. ΔE_{H^*} is calculated as $\Delta E_{\text{H}^*} = E_{\text{tot}} - E_{\text{sub}} - 1/2 E_{\text{H}_2}$, where E_{tot} and E_{sub} are energies of H adsorbed system and the clean given surface, and E_{H_2} is the energy of H_2 molecular in gas phase.

Electrocatalytic hydrogen evolution measurement

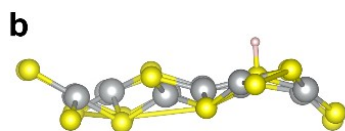
The electrocatalytic hydrogen evolution performance of NiS_x was evaluated on a CHI660E electrochemical workstation. Electrochemical analysis was performed using a standard three-electrode system, which contains a working electrode (a glassy carbon electrode loaded with 0.21 mg/cm² catalysts), a reference electrode (a Hg/HgO electrode) and a counter electrode (a Pt wire). 0.5 M H₂SO₄ was applied as electrolyte. An electrochemical activation process was firstly scanned in cyclic voltammetry from 0 to 0.9 V (vs. Hg/HgO) for 5 circles. Then, the linear sweep voltammetry (LSV) for HER was acquired at the scan rate of 5 mV s⁻¹. Finally, all measured potentials are converted to reversible hydrogen electrode (RHE) potentials according to the Nernst equation ($E_{(RHE)} = E_{(Hg/HgO)} + 0.098V + 0.059 \times pH$).

Table S1. The phase structure and crystal cell parameters of NiS_x.

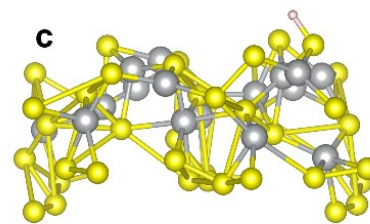
Sample	Crystal Phase	Space Group	a (nm)	c (nm)	V (nm³)
h-NiS	hexagonal	P6 ₃ /mmc	0.342	0.528	0.0267
t-NiS	trigonal	R3m	0.963	0.315	0.126
c-NiS ₂	cubic	Pa $\bar{3}$	0.567		0.182



Hexagonal phase



Trigonal phase



Cubic phase

Figure S1. Optimized atomic structures of phase-engineered NiS_x adsorbed with H atom.

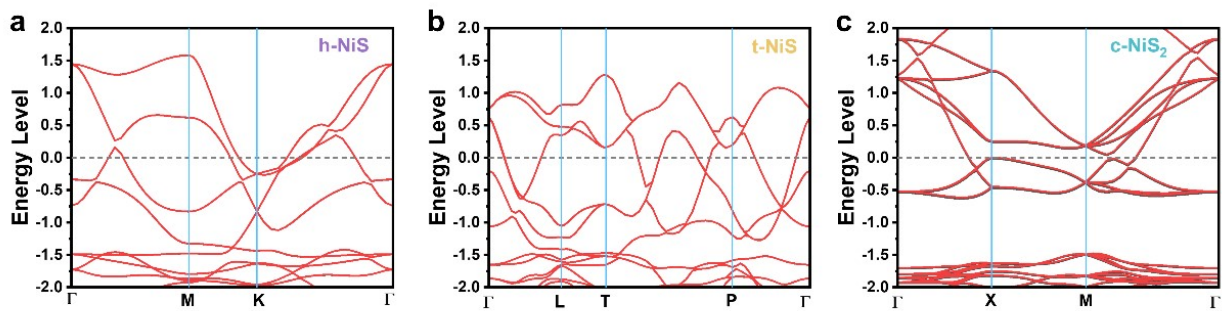


Figure S2. Calculated band structures of h-NiS, t-NiS and c-NiS₂.

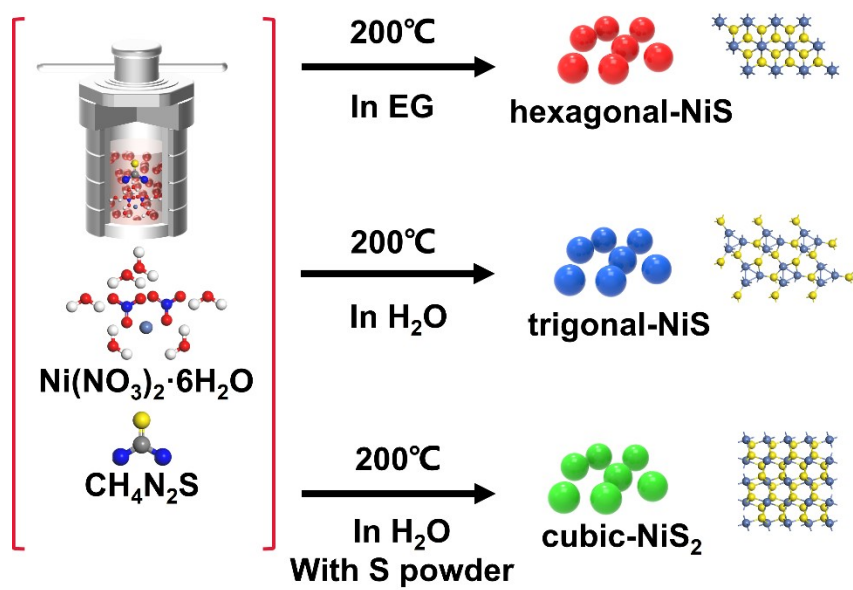


Figure S3. Synthetic processes of phase-engineered NiS_x.

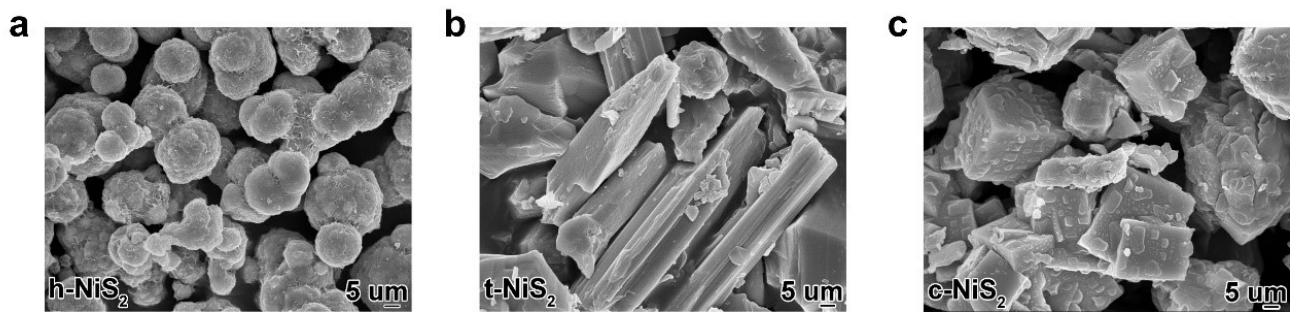


Figure S4. SEM images of h-NiS, t-NiS and c-NiS₂.

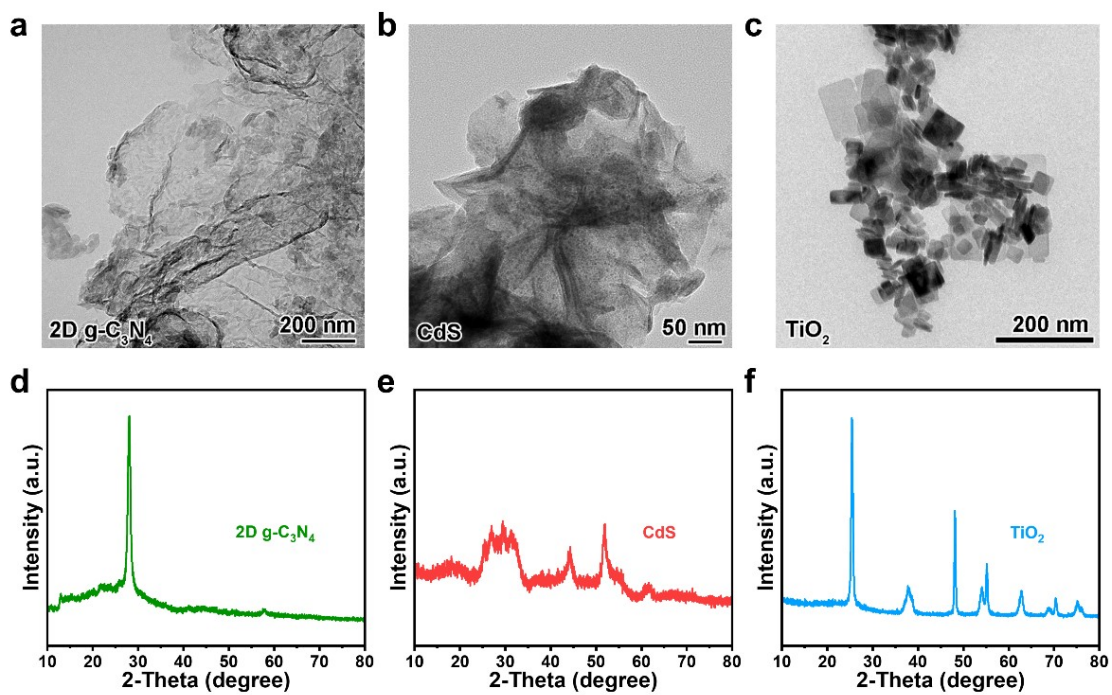


Figure S5. (a-c) TEM images of CN nanosheets, CdS nanosheets and TiO₂ nanosheets. (d-f) XRD patterns of CN nanosheets, CdS nanosheets and TiO₂ nanosheets.

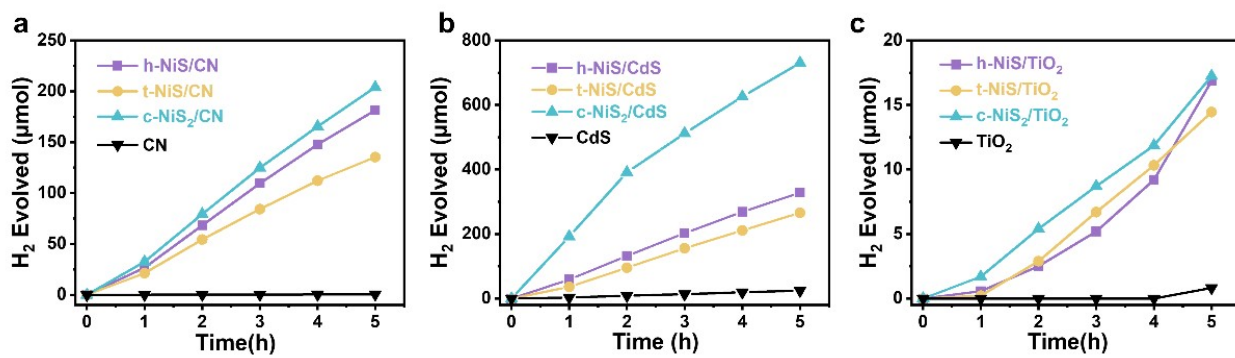


Figure S6. Time-dependent hydrogen evolution performance of the catalysts.

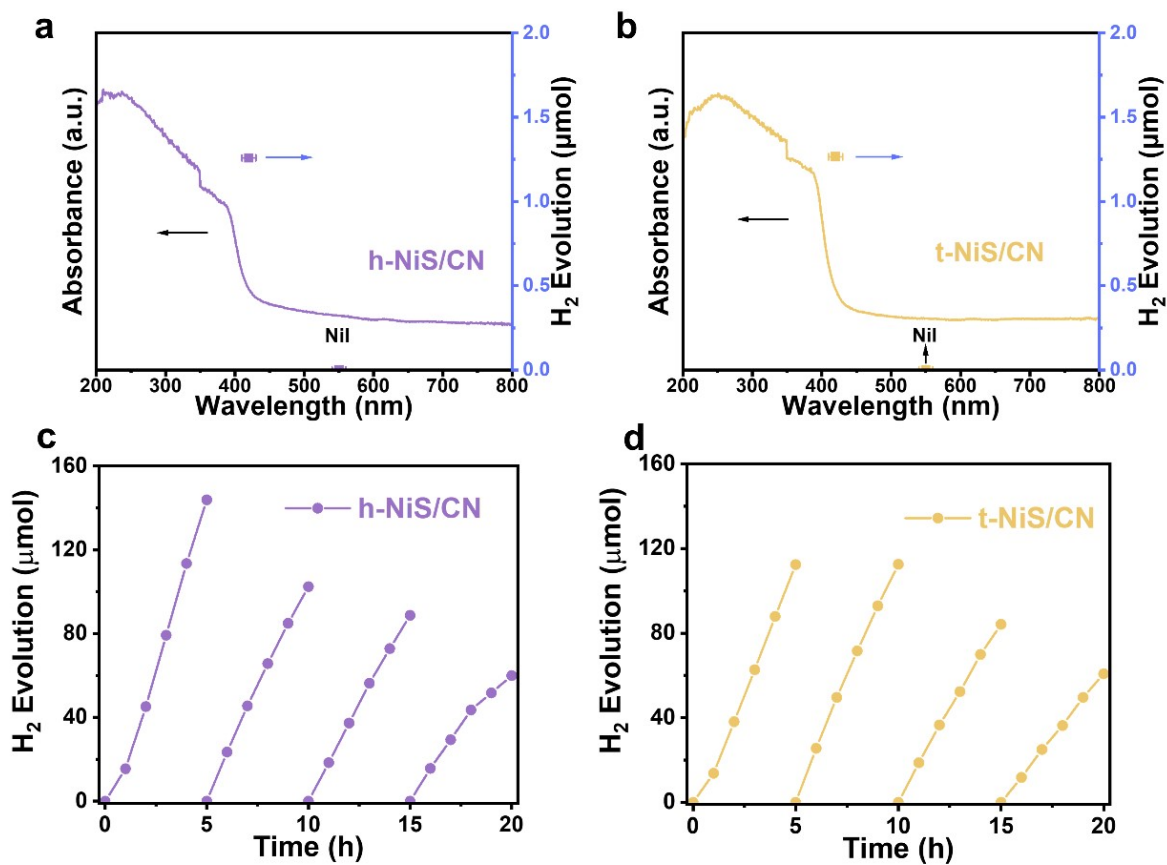


Figure S7. (a-b) Wavelength-dependent hydrogen evolution performance of h-NiS/CN and t-NiS/CN. (c-d) Catalytic stability tests of h-NiS/CN and t-NiS/CN.

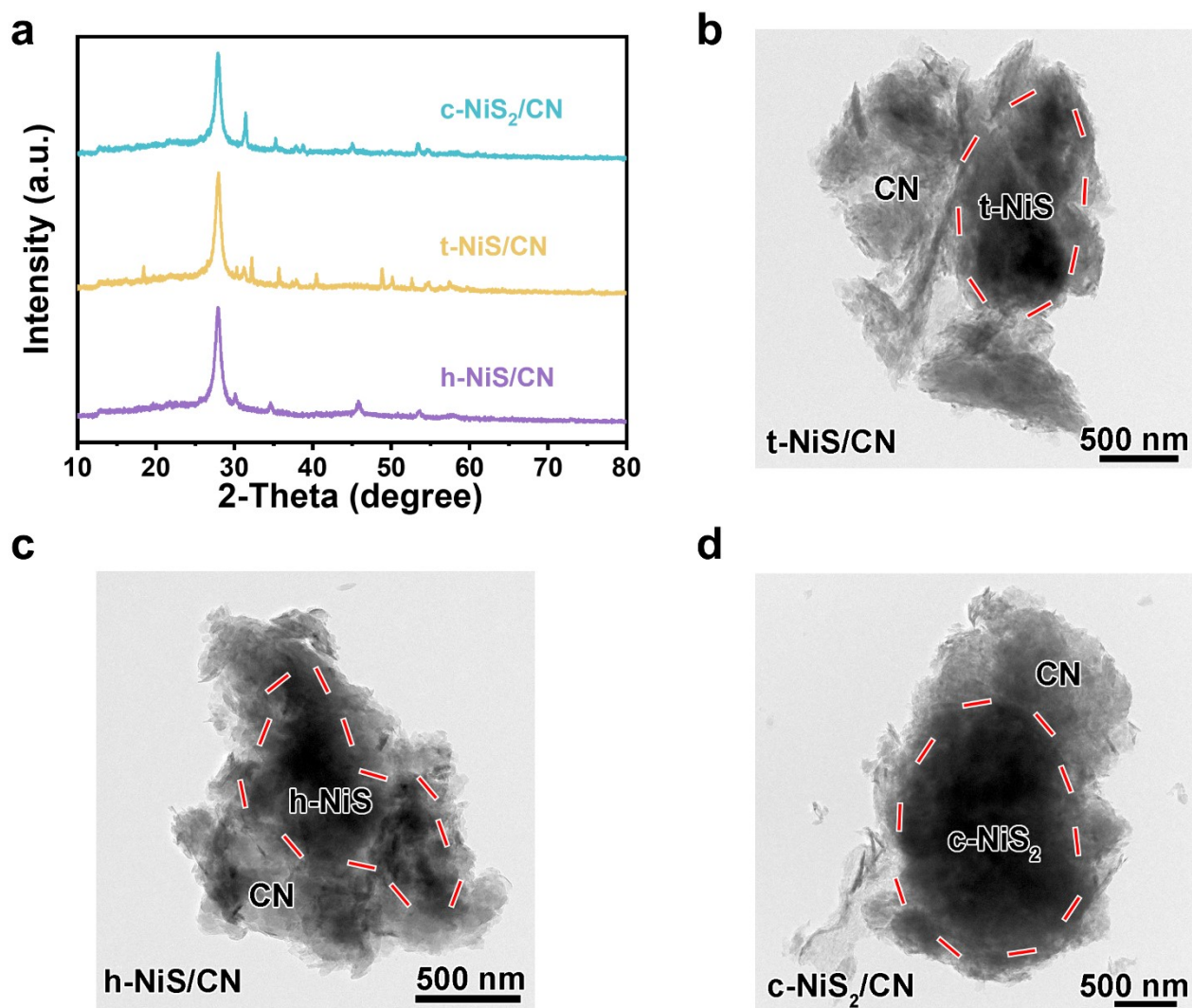


Figure S8. (a) XRD patterns and (b-c) TEM images of h-NiS/CN, t-NiS/CN and c-NiS₂/CN

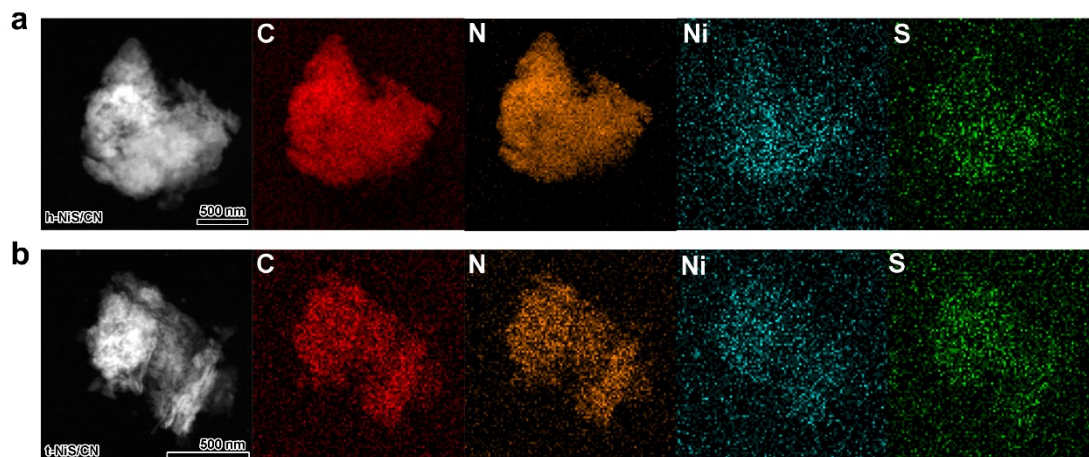


Figure S9. STEM images of corresponding elemental mapping of (a) h-NiS/CN and (b) t-NiS/CN

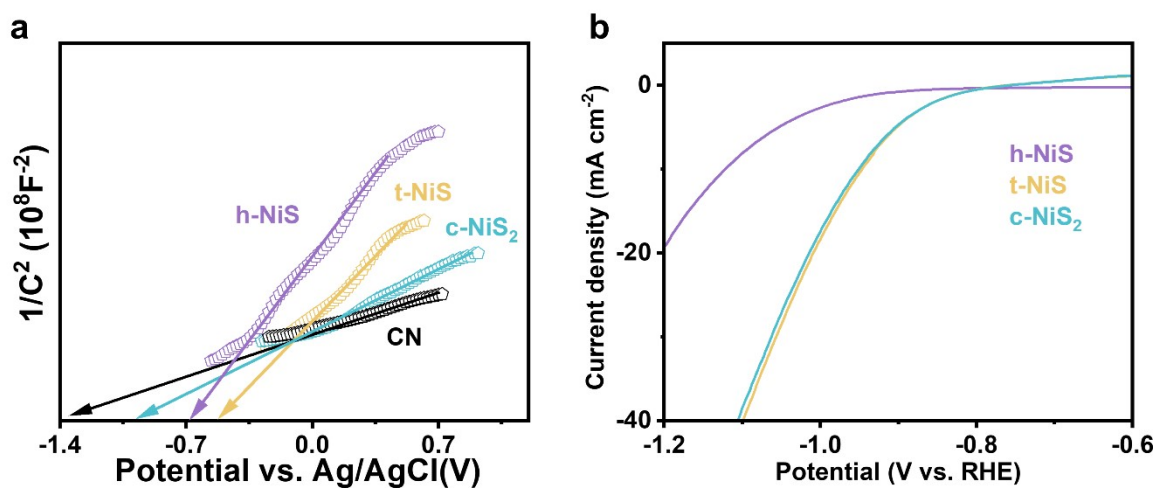


Figure S10. (a) Mot-schottky curves of h-NiS, t-NiS, c-NiS₂ and CN in 0.5 M Na₂SO₄. (b) LSV curves of h-NiS, t-NiS and c-NiS₂ in 0.5 M H₂SO₄.

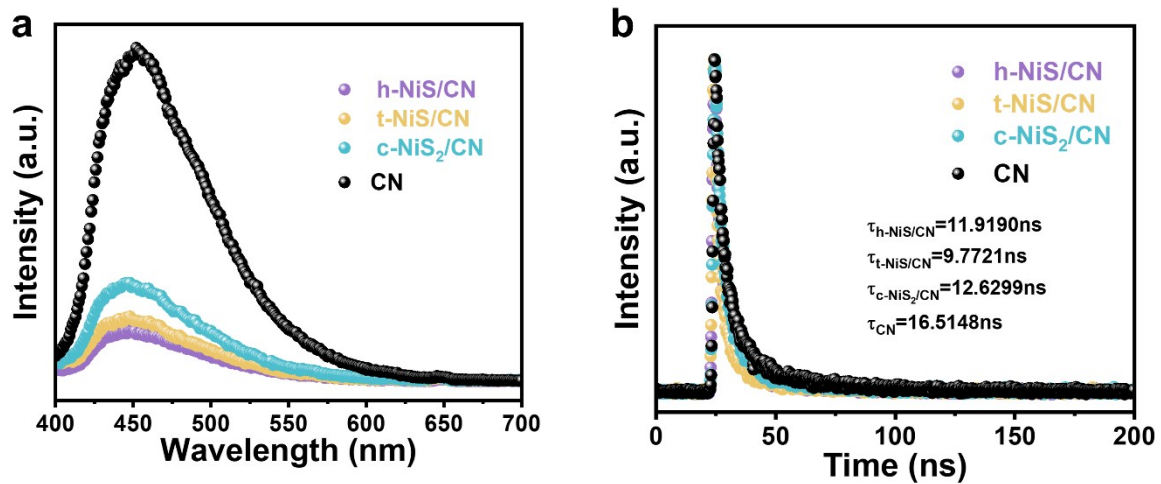


Figure S11. (a) Steady-state and (b) transient-state fluorescence spectra of CN, h-NiS/CN, t-NiS/CN and c-NiS₂/CN.

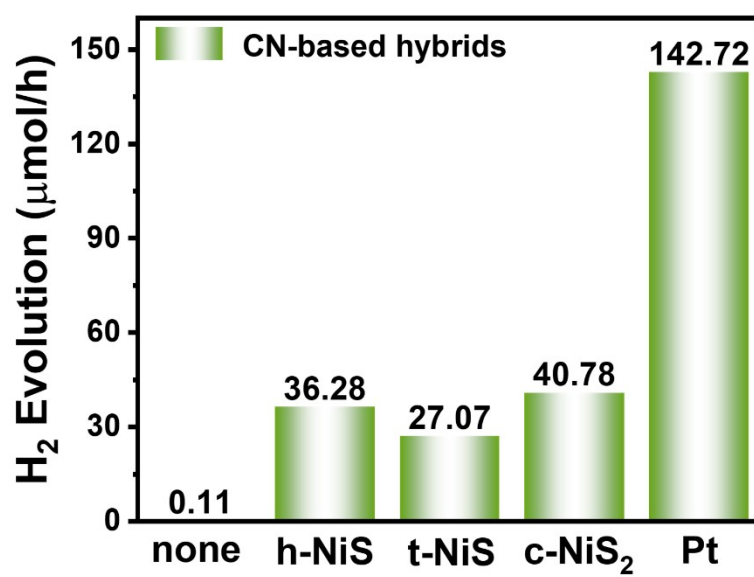


Figure S12. performance comparison between Pt and phase-engineered NiS_x using CN as hosting semiconductor.